Climate Dynamics (2024) 62:187–201
https://doi.org/10.1007/s00382-023-06909-1

The weakening of the tropical circulation is caused by the lifting of the tropopause height

Chen-Shuo Fan[1] · **Dietmar Dommenget**[1]

Received: 20 March 2023 / Accepted: 29 July 2023 / Published online: 9 August 2023

Abstract
In this study we analyse the physical processes causing the weakening of the tropical circulation in the Coupled Model Intercomparison Project 6 (CMIP6). We apply a diagnostic model for the large-scale tropical circulation (vertical motion) based on the moist static energy for the first baroclinic mode (MSEB) and evaluate the sensitivity of the tropical circulation changes to the changes in advection of moisture and heat, the net radiation, the moist static stability, the baroclinic mode, and to the height of the tropopause. Based on the CMIP6 model simulations we find that the tropical circulation weakens by about 10-15% over the twenty-first century. The analysis of the MSEB model suggests that the primary cause for this weakening of the tropical circulation is the lifting of the tropopause height. This effect is fairly uniform throughout the tropics and present in all model simulations. The tropopause height increase shifts the first baroclinic mode away from lower levels with unstable air masses into high levels of the troposphere where stable air masses lead to a stabilisation of the large-scale circulation. Other factors such as changes in the advection of moisture and heat, increased net heating or increased instability of the lower tropospheric gross moist stability do have strong regional differences, and mostly increase tropical circulations, counteracting the weakening caused by the lifting of the tropopause.

Keywords Tropical circulation · Global warming · Moist static energy · Diagnostic model

1 Introduction

Changes in the hydrological cycle caused by global warming are vital to society. Achieving a reliable precipitation projection remains a major challenge (IPCC 2021). Rising carbon dioxide concentrations are anticipated to influence the hydrological cycle via increases in global mean temperature and atmospheric water vapor content (Held and Soden 2006). However, precipitation changes in the tropics are also dependent on the tropical circulation (Held and Soden 2006; Vecchi and Soden 2007). In climate model simulations of global warming, a weakening of tropical circulation is observed (Vecchi and Soden 2007; Tokinaga et al. 2012; Hu et al. 2018). The purpose of this paper is to use the moist static energy equation for first baroclinic mode (MSEB) model by Fan and Dommenget (2021) as a diagnostic tool to look into the causes of the weakening circulation.

Evidence for the decrease in strength of the large-scale tropical circulation under global warming was presented by Held and Soden (2006) based on analyzing the changes in mass flux to balance precipitation and evaporation rates. They found a robust decrease in convection mass flux from Coupled Model Intercomparison Project 3 (CMIP3) in climate change experiments, suggesting a weaker tropical circulation. This general slowdown of the circulation is also found in both the Walker (Tokinaga et al. 2012; DiNezio et al. 2013; Wu et al. 2021) and the Hadley circulation of both hemispheres (Mitas and Clement 2006; Hu et al. 2018; Xia et al. 2020).

Studies aiming at understanding the causes of the tropical circulation changes or the theoretical aspects of it mostly focus on aspects of the moist static energy (MSE) balances of the tropical troposphere. For instance, recent studies found that increased surface warming due to carbon dioxide forcing slows down the tropical circulation and is dominated by the increase in static stability in the troposphere (Chou et al. 2013; Plesca et al. 2018a). In further studies,

✉ Chen-Shuo Fan
chen-shuo.fan@monash.edu

[1] ARC Centre of Excellence for Climate Extremes, School of Earth Atmosphere and Environment, Monash University, Clayton, VIC 3800, Australia

the increased atmospheric stability has also been used to explain regional weakening responses such as Walker circulation (Wills et al. 2017; Duffy and O'Gorman 2023) and Hadley circulation (Feldl and Bordoni 2016; Chemke and Polvani 2021).

A series of studies (Chou and Chen 2010; Chou et al. 2009, 2013) have used the conservation of the MSE to examine projected changes in the tropical circulation. The MSE budget framework considers the net heat flux (including radiative effects) from surface and top of atmosphere (TOA), air column stability, and horizontal energy transportation. Under global warming, low-level temperatures and moisture increase, increasing MSE import, which must be counterbalanced by a rise in MSE export at higher levels. This is done by increasing both the height of convective outflow and the rate at which air at higher levels warms up.

Chou et al. (2013) implied that the increased gross moist stability (GMS) (i.e., a more stable atmosphere) is consistent with the weakening of circulation found in climate models and were able to point out that the rising tropopause is crucial for this response. Wills et al. (2017) further investigated how the GMS constrains changes in the Walker circulation strength across a wide range of climates in idealized general circulation model (GCM) simulations and showed that the GMS increases with warming, mostly because the height of the tropopause goes up. Recently, a study using the MSE budget by Duffy and O'Gorman (2023) supported a strong relationship between changes in Walker circulation and GMS. Feldl and Bordoni (2016) used simulations from a collection of coupled GCMs to quantify changes in Hadley cell strength and discovered that the weakening of the Hadley circulation is characterized by an increase in stationary and transient eddy heat flux, an increase in GMS, and a change in the temperature profile. While recent work by Kim et al. (2022), based on a coupled GCM, indicated that the key factor for changes in Hadley circulation is not GMS but the radiative forcing effect under the MSE framework, the study provides a different perspective on understanding the mechanisms behind these circulation changes.

Despite the importance of GMS, there remains a paucity of discussion about the contributions from GMS and other components (e.g., detailed constraints of GMS, heat flux, MSE advection) to the overall weakening of the tropical circulation. In addition, although projections under the warming scenario almost concurrently indicate a circulation weakening, there is still a degree of variation in circulation weakening (Vecchi and Soden 2007). Insufficient understanding of the circulation dynamics, according to previous studies (Plesca et al. 2018b; Duffy and O'Gorman 2023), diminishes full confidence in such a response (i.e., weakening of the Walker circulation).

Overall, some previous research on the changes in tropical circulation due to global warming made extensive use of the MSE budget in their analysis and emphasized the significance of GMS in circulation change research. However, this has yet to lead to a comprehensive understanding of the underlying factors driving the weakening of global tropical circulation under a warming scenario, and an in-depth analysis of the contributions to circulation changes when integrating the MSE budget and the GMS perspective is needed.

Recently, a diagnostic model for the large-scale tropical circulation (vertical motion) based on the moist static energy equation for first baroclinic mode anomalies (MSEB model) was proposed by Fan and Dommenget (2021) (hereafter FD21), which combines the MSE budget and GMS. The MSEB model is based on previous studies relating vertical motion in the tropics to the driving forces of the tropospheric column heating rate, advection of moisture and heat, and the moist stability of the air columns scaled by the first baroclinic mode. The model is capable of diagnosing the large-scale pattern of vertical motion of the mean state, the annual cycle, interannual variability, model-to-model variations, and in warmer climates of climate change scenarios.

This paper aims to apply the MSEB model to provide a comprehensive and general understanding of the physical causes of the weakening tropical circulation. We will provide a detailed sensitivity analysis of all elements in the MSEB model that drive the changes in the tropical circulation. The analysis will clearly illustrate how the lifting of the tropopause height is causing the weakening of the tropical circulation, while at the same time we illustrate how all other elements of the MSEB model contribute to tropical circulation changes.

The remaining part of this study proceeds as follows. Section 2 will describe the model outputs, such as CMIP6 simulations under historical and climate change scenarios, and the analysis methods used in this study. This will also give a short introduction into the MSEB model. In Sect. 3, we will quantify the weakening of the tropical circulation based on the CMIP6 model ensemble, which will be followed by a detailed sensitivity analysis of the MSEB model to highlight the causes of this weakening in the tropical circulation in Sect. 4. This study will be concluded with a summary and discussion in Sect. 5.

2 Data and methods

2.1 Model data

Our analysis is based on the newest released CMIP6 dataset of ocean-atmosphere coupled climate models for historical and SSP5-8.5 (i.e., warming scenario) simulation (O'Neill et al. 2016; Eyring et al. 2016). We use all models with the necessary data fields for this study and analyze only one ensemble member from each CMIP model.

All data from the CMIP6 outputs is extracted as monthly mean values on surface and pressure levels (14 pressure levels, 1000-30 hPa), then interpolated to 3.75° × 3.75°. The data period from the CMIP historical simulation is from 1979 to 2014, and the data period from the CMIP SSP5-8.5 simulation is from 2015 to 2099. The single-level variables include surface latent heat flux, surface sensible heat flux, and surface/top upwelling/downwelling solar/thermal radiation. The multi-layer variables include vertical velocity, U-component of wind, V-component of wind, specific humidity, temperature, and geopotential.

All calculations for the MSEB model are done on the original data/model grids, and the MSEB model outputs are monthly three-dimensional vertical velocities on the native resolution of CMIP6 models. These outputs are then interpolated onto a common 3.75° × 3.75° grid for analysis. Throughout the analysis, we define the tropical region as latitudes less than or equal to 30° from equator. For testing MSEB model on different boundary settings (e.g. ocean-only), we used land-sea mask which is based on Rand's Global Elevation and Depth Data (RAND Corporation 1980).

2.2 Moist static energy equation for first baroclinic mode (MSEB) model

In this paper, we apply the MSEB model (FD21) as a diagnostic tool to estimate tropical circulation, as approximated by the 500-hPa vertical pressure tendencies, ω. The MSEB model approximates ω by

$$\omega \approx \frac{-g}{GMS_B}(Adv + F_{net}) \tag{1}$$

with g as the global gravity constant. F_{net} is the net energy flux into the air column by surface latent and sensible heat, and by short and long wave radiation. Following Chou et al. (2013) Adv is the vertically-integrated advection of moisture and heat into the air column:

$$Adv = -\langle \boldsymbol{v} \cdot \nabla \left(L_v q + C_p T\right) \rangle_{P_T} \tag{2}$$

The vertical integral $\langle\rangle_{P_T}$ denotes a mass weighted vertical integration from surface to the tropical mean tropopause height, P_T. P_T is defined as the height at which the lapse rate is 0 °C/km (Gettelman et al. 2009). The lapse rate is calculated based on spline fit method with about 25 m resolution for tropical mean temperature profile. The performance of the MSEB model is quite sensitive to the definition of tropopause height. While, the results of this studies are fundamentally not altered if we use the above definition of all CMIP models, for 9 out of the 31 models (9, 10, 11, 16, 20, 21, 24, 29, 30 in Table 1) the MSEB models estimates have less spread between the CMIP models if we use a lapse rate of +2 °C/km to define P_T. We therefore present the results here for 22 models with the 0 °C/km and 9 models with the +2 °C/km criteria. The q and T are the specific humidity and air temperature. The constant of L_v, and C_p are the latent heat of vaporization, and the specific heat at constant pressure, respectively. $\boldsymbol{v}$ is the horizontal wind field and ∇ denotes the horizontal gradient operator. In the MSEB model, F_{net} and Adv are horizontal fields of tropospheric integrals. The GMS_B is the gross moist stability (GMS) weighted by the first baroclinic mode Ω:

$$GMS_B = \frac{M}{\Omega} \tag{3}$$

With M defined as the gross moist stability (GMS):

$$M = -g\langle \Omega \partial_p h \rangle_{P_T} \tag{4}$$

where ∂_p is vertical gradient operator in pressure coordinate and h represents MSE defined as

$$h = C_p T + L_v q + gz \tag{5}$$

Table 1 List of CMIP6 models

No.	Model	No.	Model	No.	Model
1	TaiESM1	12	CNRM-ESM2-1	23	UKESM1-0-LL
2	AWI-CM-1-1-MR	13	EC-Earth3	24	MPI-ESM1-2-LR
3	BCC-CSM2-MR	14	EC-Earth3-CC	25	MRI-ESM2-0
4	CAMS-CSM1-0	15	EC-Earth3-Veg	26	CESM2-WACCM
5	FGOALS-f3-L	16	EC-Earth3-Veg-LR	27	NorESM2-LM
6	FGOALS-g3	17	FIO-ESM-2-0	28	KACE-1-0-G
7	CanESM5	18	INM-CM4-8	29	NorESM2-MM
8	CMCC-CM2-SR5	19	INM-CM5-0	30	GFDL-CM4
9	CMCC-ESM2	20	IPSL-CM6A-LR	31	GFDL-ESM4
10	CNRM-CM6-1	21	MIROC-ES2L	32	NESM3
11	CNRM-CM6-1-HR	22	MIROC6		

it combines air parcel's enthalpy (C_pT), latent energy (L_vq), and potential energy (gz) with z as the geopotential height. Ω represents the first baroclinic mode, which to first order represents the vertical structure of vertical motion in the tropics. It is calculated based on the tropical mean temperature profile and tropopause height assuming a convective quasi equilibrium and hydrostatic atmosphere, integrating the vertical structure of the baroclinic wind from surface to the tropopause height (Wills et al. 2017). In the MSEB model, GMS_B and h are three-dimensional fields (a function of x, y and z), and M is a horizontal field of a tropospheric integral and Ω is a mean vertical profile.

In summary, ω is driven in the MSEB model estimate by the combined F_{net} and Adv, where a net gain (loss) in moist statistic energy due to these two terms lead to upward (downward) motion. The sensitivity of ω to these two drivers is determined by GMS_B, which is positive (stable) for all the cases examined in this study. Smaller (larger) values of GMS_B, lead to a larger (smaller) sensitivity of ω to F_{net} and Adv. In turn, for given F_{net} and Adv fields smaller (larger) values of GMS_B, lead to an intensification (weakening) of the ω field. In the following analysis we will only discuss the 500 hPa level of ω and GMS_B.

2.3 Sensitivities of the (MSEB) model

In the MSEB model we can estimate the sensitivity of ω to the elements on the RHS of Eq. (1). For these sensitivity experiments, the historical climate during 1970–1999 is the control (hereafter HIS) scenario, and the future climate during 2070–2099 is the SSP5-8.5 warming (hereafter SSP) scenario. For instance, if we like to evaluate the sensitivity of the changes in ω from the HIS to SSP scenario to the F_{net} forcing term, we can compute ω based on Eq. (1) with all elements of the RHS from the HIS scenario, but use the SSP values only for F_{net}. The difference to the MSEB model with all elements of the RHS from the HIS scenario provides an estimate of the sensitivity of the changes in ω to the change in F_{net}. In the following study we will discuss a series of such sensitivity analysis, in which we evaluate the changes in one element of the RHS of Eq. (1) at a time. The elements that we discuss are: GMS_B, F_{net}, Adv, Ω, $\partial_p h$, P_T, and T. It should be noted here, that the sum of the individual sensitivity experiments is not expected to explain the total change, since the elements of Eq. (1) are not a linear function for all terms.

3 The weakening of the tropical circulation

We start the result sections with the analysis of the CMIP6 simulations and how they represent the changes of the large-scale tropical circulation with a focus on the weakening of the circulation.

Figure 1 shows the ensemble mean vertical circulation in the CMIP simulation of the HIS and SSP scenarios. In both simulations we can notice similar large-scale structures of the tropical circulation, with ascending motions dominant near the equator and descending motions dominate over the subtropical regions, highlighting the large-scale Hadley circulation. We can further notice the strong contrast between ascending and descending along the equatorial regions, in particular in the Pacific highlighting the Walker circulation cells.

By comparing the mean vertical circulation in the HIS and SSP scenarios we can notice that the large-scales features are generally weaker in the SSP than in the HIS simulation, indicating a weakening of the large-scale circulation. This includes a weakening of both the Hadley and Walker circulations, but also holds more generally. It also holds for both oceanic and land regions. The linear regression of the SSP ensemble tropical mean onto the HIS ensemble mean has a slope of 0.85, suggesting that the large-scale circulation of the HIS simulations exist in the SSP scenario with an amplitude that is about 15% weaker than in the HIS simulations.

The response difference between HIS and SSP scenarios is shown in Fig. 1c. The pattern is similar to the mean circulation, but reversed sign, indicating a weakening of the circulation. However, the correlation between the response pattern and the HIS mean circulation pattern is only −0.57, suggesting that the 32% of the response can be consider a linear decrease of the HIS mean circulation. In turn, about 68% may not be described as a weakening of the mean circulation, but a change in the pattern of the large-scale circulation. One of the most prominent features in this pattern can be noted in the central equatorial Pacific, which is related to an eastward shift of the Walker circulation (e.g., Bayr et al. 2014).

A general approach to estimate the strength of the tropical circulation is to compute the root-mean-square (RMS) of the mean circulation. This allows an objective quantification of the strength of the mean ascending and descending motion irrespective of how they would relate to the HIS simulations (see values in Fig. 1). This metric considers the magnitude of circulation in both convective and non-convective regions, unlike Vecchi and Soden (2007), who only consider circulation intensity in convective regions (ascending motions). Thus, a decrease in the RMS reflects a weakening of the circulation as a whole. It does not assume a fix circulation pattern, but also considers any change (shift) in the mean circulation.

Figure 2 shows the relative change in the RMS for the SSP scenarios for oceanic and land regions. The ensemble mean shows a very clear decreasing of the tropical oceans mean circulation by about 10–15% by the end of twenty-first century relative to 1970–1999 in the HIS simulation,

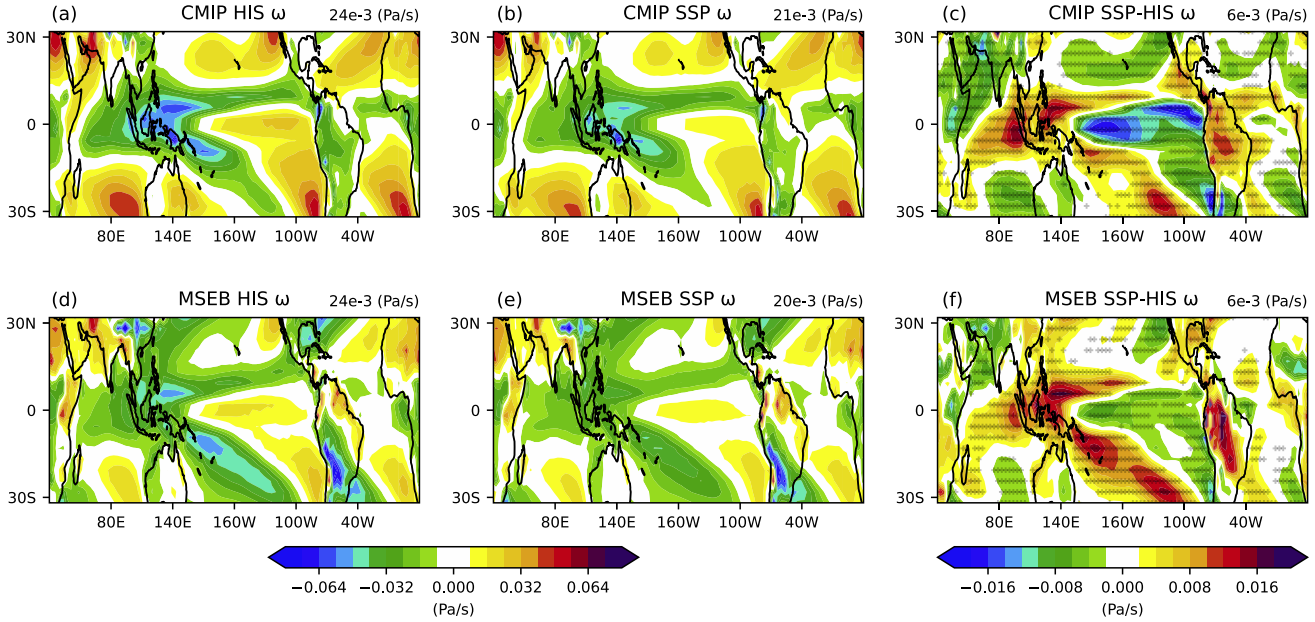

Fig. 1 CMIP6 ensemble mean (31 models) of ω (upper panels) and corresponding results based on the MSEB model (lower panels). From left to right, they are the annual mean ω in the historical scenario (1970–1999), annual mean ω in the warming scenario (2070–2099), ω change from SSP5-8.5 warming scenario data minus historical scenario data. The stippling indicates that over 22 (70%) models agree with the change of the sign. Positive (negative) values represent vertical motion in a downward (upward) direction. The RMS values are shown in the heading of each panel

consistent with previous studies (Bony et al. 2013; Kjellsson 2015; Huang et al. 2017). There is some spread within the model ensemble, but all models indicate a decrease in the strength of the mean tropical atmospheric circulation over the oceanic region. The result is similar over land, but the signal is weaker and less clear, with some models not showing a declining circulation over land.

4 Sensitivity analysis with the MSEB model

We now focus on what is driving the weakening of the tropical circulation, by using the MSEB model as a diagnostic tool. We will first illustrate the fidelity of the MSEB model and then focus on a sensitivity analysis of the MSEB model to the different forcing terms in the model.

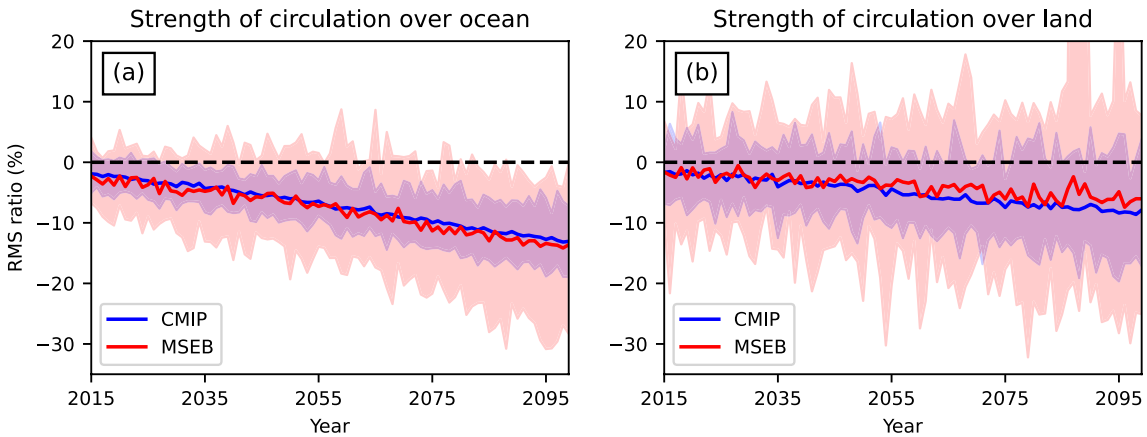

Fig. 2 Time series (2015–2099) of the annual mean RMS change of ω over the tropical ocean (left) and land (right) between 31 CMIP6 model outputs and MSEB model estimations. The RMS is the circulation changes under a warming scenario in percentage in reference to a period of historical simulation data (1970–1999). Color lines represent the ensemble mean of different cases (see legend). A color-filled region indicates a region between the minimum value and maximum value along with the y-axis of all ensemble members

4.1 Assessment of the MSEB model's performance

The MSEB model estimate of the CMIP tropical mean circulation and its change are shown in Fig. 1d–f in comparison with CMIP circulations. In general, the MSEB model captures the mean large-scale circulation of the CMIP models well, which will be quantified in the follow analysis (i.e., in Fig. 3). There are, however, some deficiencies that can be noted. For instance, the MSEB model underestimates the descending over the Pacific cold tongue, it has a bias towards upward motions at higher latitudes and the mismatch over land regions is stronger than over oceans. These limitations have been attributed to various factors in FD21, including the model's assumption of convective quasi equilibrium, its reliance on a tropics-wide constant first baroclinic mode, and the low temporal resolution employed for calculations in the advection terms.

The MSEB model estimate also captures the main features of the weakening of the tropical circulation. The SSP mean tropical circulation is generally weaker than the HIS circulation (Fig. 1d, e) and the response pattern is again negatively correlated (–0.64) with the HIS mean circulation pattern, indicating that the change in the circulation is partially a weakening of the HIS circulation. The RMS

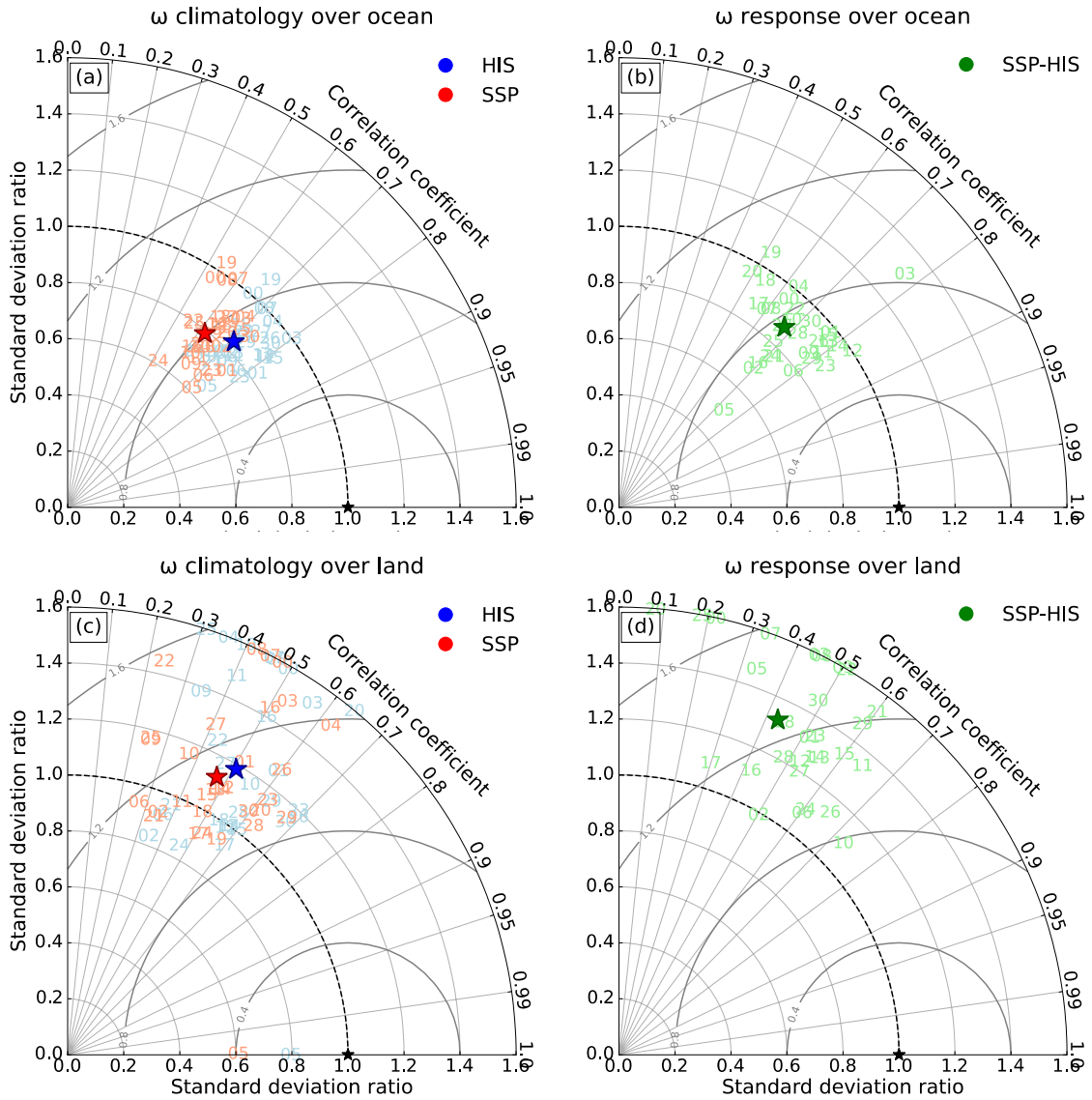

Fig. 3 Taylor diagram (MSEB model's estimation vs. CMIP6 model output) of ω based on 31 CMIP6 model outputs over the tropical ocean (upper panels) and land region (lower panels). **a**, **c** Climatological ω in historical and warming scenarios (see legend). **b**, **d** ω change from warming scenario data minus historical scenario data. The numbers represent each individual model in Table 1. The stars represent the average of 31 models

decrease of the tropical mean circulation over ocean regions as estimated by the MSEB model is nearly identical to those of the CMIP model, but it does have some wider spread within the model ensemble (Fig. 2a). Over land the MSEB model shows a larger disagreement with the CMIP models, with a much weaker decrease in the RMS and wide spread within the model ensemble.

Figure 3 depicts Taylor diagrams to quantify the performance of the MSEB model. Over oceans the MSEB model estimate of the mean HIS circulation has a spatial correlation between 0.6 and 0.8 for most model and the amplitude of the circulation (standard deviation) is weaker than the CMIP mean circulations (Fig. 3a). This illustrates a good representation of the HIS circulation. The performance is slightly less good for the SSP simulations, but is still of similar quality. There is a tendency of the MSEB models to underestimate the strength of the circulation (ensemble mean standard deviation ratio is smaller than 1.0; Fig. 3a). The performance on estimating the oceanic response pattern is of similar quality than for the HIS and SSP, but it does show some wider spread in the pattern correlation within the ensemble and the overall amplitude is again underestimated (ensemble mean standard deviation ratio is slightly lower than 1.0; Fig. 3b).

The performance of the MSEB model over land regions is substantially worse than over oceans (Fig. 3c, d) for the HIS, SSP and response pattern. The pattern correlation is only moderate with values ranging between 0.2 and 0.7 and pattern amplitude is overestimated, in some models by more than 50%. This marks a substantial limitation of the MSEB model. According to previous investigation in FD21, this issue is somewhat linked to regions with higher topography (e.g., the Andes in South America or the Himalaya in Asia).

In summary, our analysis leads us to the conclusion that the MSEB model effectively captures the tropical mean atmospheric circulation and its changes as the climate warms over oceanic regions. However, it exhibits limited skill when applied to land regions. Due to the problems over land we will focus our following discussion on ocean regions only. While much of the discussion may be similar over land, we will not discuss the land response given the MSEB model limitations.

4.2 Drivers of the weakening of the tropical circulation

Figure 4 shows the relative RMS change for the tropical circulation over oceans for the CMIP6 ensemble and the MSEB estimate for the last 30 years of the twenty-first century. In addition, sensitivity estimates of the MSEB model are shown in which only one of the driving terms is altered from the HIS to the SSP values (see methods section for details). It should be noted that the total MSEB change does not equal to the sum of the contributions from the F_{net}, Adv and GMS_B terms, since they are not linear elements of Eq. (1).

We can note that the F_{net} and Adv terms both would intensify the tropical circulation, while the GMS_B is the only driver responsible for an overall weakening of the tropical ocean circulation, acting against the tendencies of the F_{net} and Adv terms. The dominant role of the GMS in driving the weakening of the tropical circulation is consistent with previous studies (Chou et al. 2013; Feldl and Bordoni 2016; Wills et al. 2017; Plesca et al. 2018a; Duffy and O'Gorman 2023). A recent study by Duffy and O'Gorman (2023), focusing on the weakening of the Walker circulation in the Pacific, suggests that F_{net} contributes to amplifying the weakening effect. This contrasts with our findings for the whole tropics that F_{net} contributes to the intensification of tropical circulation. It implies that F_{net} has a strong effect on intensifying tropical circulation outside of the equatorial Pacific region.

More detailed maps of the local changes in F_{net}, Adv and GMS_B from the HIS to SSP simulation are shown in the left column of Fig. 5. The right column shows the sensitivity of the tropical circulation in the MSEB model to each other these terms. Starting with the radiation term F_{net} we can see substantial and complex changes, which have significant impacts on the tropical circulation patterns (Fig. 5a, b). Changes in F_{net} lead to both regional intensifications and weakening of the tropical circulation. In the Indo-Pacific warm pool and the Pacific equatorial cold tongue the F_{net} changes drive weakening of the circulation, whereas in most other regions it drives a strengthening of the circulation. In particular, in the east tropical Indian Ocean and most of the tropical Atlantic. The impact of F_{net} is mostly in the deep tropics and less so on higher latitudes.

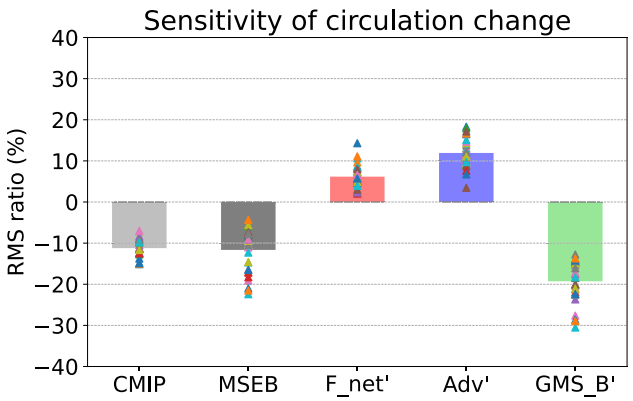

Fig. 4 Ensemble mean changes in the RMS of ω for the tropical ocean based on CMIP6 model outputs, MSEB model estimations, and three sensitivity experiments (see x-axis labels). The detailed sensitivity method is described in Sect. 2.3. The symbol of the triangle represents each individual climate model

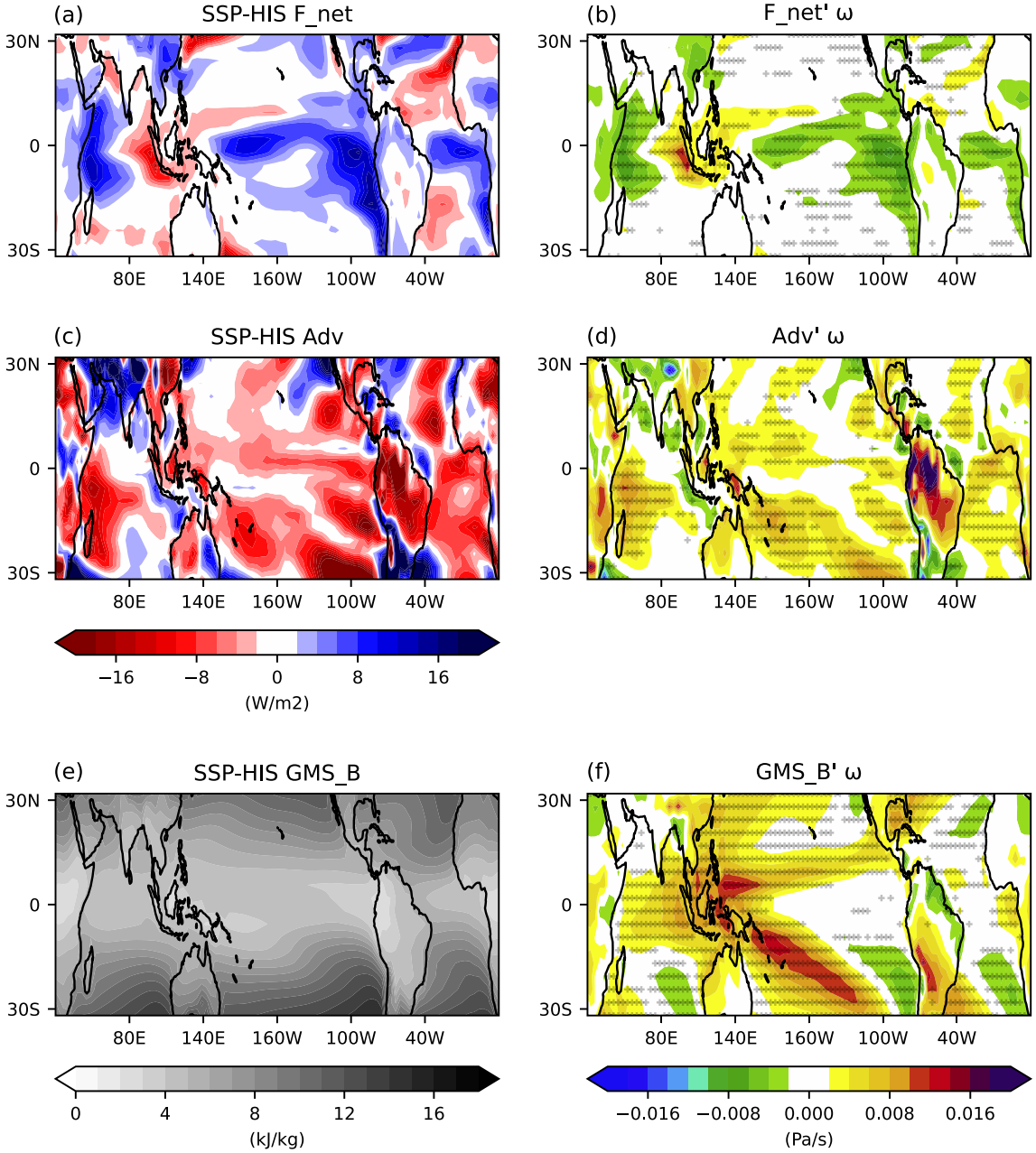

Fig. 5 Elements of the MSEB model: left column: ensemble mean changes (scenario minus historical) based on 31 CMIP6 model outputs for F_{net} (top), *Adv* (middle), GMS_B (lower). Right column: Corresponding MSEB model sensitivity of ω sensitivity to each element shown on the left-hand side. The stippling indicates that over 22 (70%) CMIP6 models agree with the change of the sign

Results from previous studies are consistent with the F_{net} changes found here. Su et al. (2014) found that a rising altitude of convection and cloud tops causes an increase in the longwave warming effect of clouds. This effect causes net energy heat flux at TOA (F_{top}) to increase. Equatorial SST warming can influence wind-evaporation-SST feedback in the tropics (Xie et al. 2010; Long et al. 2016), which increases the surface latent heat flux, resulting in a decrease in net energy heat flux at surface (F_{sur}). Both changes in TOA and surface can further result in increasing F_{net} in the deep tropics. Through comparing changes in TOA net cloud radiative effect and surface latent heat flux with the F_{top} and F_{sur} in the MSEB model, respectively, we find both comparisons show quite similar spatial distributions to previous studies (not shown).

The advection of moisture and heat (*Adv*) also has substantial impacts and is mostly acting to enhance descending motions (Fig. 5c, d). In particular, in the west Pacific

subtropical convergence zone the enhance descending motions by the *Adv* term weaken the circulation. The results are largely consistent with the study by (Byrne and Schneider 2016). They identified steeper meridional MSE gradients at low latitude in warmer climates, primarily as a result of an increase in the specific humidity equatorward gradient, which would lead to a weakening of upward motions.

Changes in GMS_B are positive throughout the tropics, representing a stabilization of the tropical troposphere (Fig. 5e). The increase in GMS_B reduces the sensitivity of the vertical motion to the forcing terms F_{net} and *Adv* in the MSEB model (Eq. 1). This effectively leads to a weakening of the tropical circulation for most regions of the tropics (Fig. 5e). The strongest effects are on the Indo-Pacific warm pool and the west Pacific subtropical convergence zone (Fig. 5f). The GMS_B changes have the strongest impact on the tropical circulation from all three terms.

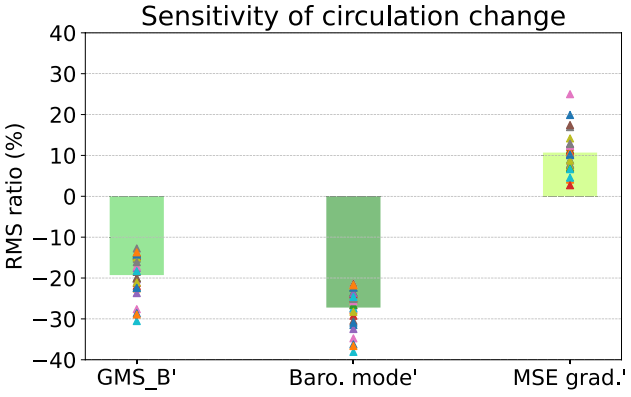

Fig. 6 Ensemble mean changes in the RMS of ω for the tropical ocean based on three sensitivity experiments (see x-axis labels). The detailed sensitivity method is described in Sect. 2.3. The symbol of the triangle represents each individual climate model

4.3 Changes in the gross moist stability

The above analysis illustrated that the driver of the tropical circulation weakening is the increase in GMS_B. The GMS_B can conceptually be thought of two main elements (Eq. 3): The baroclinic mode, Ω and the vertical MSE gradient, $\partial_p h$. Figure 6 shows the sensitivity of the RMS for the tropical circulation over oceans in the MSEB model to the main elements of the GMS_B. The change in Ω alone lead to a strong weakening of the tropical circulation of about -26%. The vertical MSE gradient, in turn, would decrease the stability of the troposphere and increase the tropical circulation by about $+10\%$. Thus, the primary cause of the weakening of the tropical circulation is the change in Ω. This finding aligns with the conclusions drawn by Duffy and O'Gorman (2023).

In the MSEB model Ω is based on a tropical mean temperature profile, and therefore is assumed to be a tropical mean mode, being the same for all tropical regions, see Fig. 7a. The mode is a top-heavy profile, with the peak between 200 and 600 hPa. This suggests that the GMS_B is most sensitive to the vertical MSE gradients at these levels of the troposphere. The Ω profile is similar in both scenarios, but it is enhanced in the SSP scenario and reaches slightly higher up. The upward shift of the top-heavy baroclinic mode is a trend towards deep convective vertical motion structure (Singh and O'Gorman 2012), and other studies have demonstrated a similar upward shift of the vertical motion structure (Chou et al. 2009; Duffy and O'Gorman 2023).

$\partial_p h$ is based on the local MSE and therefore is a three-dimensional field. The tropical mean profile over oceans is shown in Fig. 7b. In both scenarios the mean $\partial_p h$ is characterized by positive gradient profiles near the surface and negative gradient profiles at higher levels of the troposphere. This main characteristic is even more pronounced in the SSP scenario, where the positive gradient near the surface further increases and the negative gradient at higher levels also slightly decrease. The increased positive h gradient near the surface are a result of the increase in specific humidity (Duffy and O'Gorman 2023), whose rate of increase declines gradually with altitude (Richter and Xie 2008). The increased negative h gradient of the upper atmosphere are attributable to latent heat release from deeper convection and the radiative effect of cloud change, resulting in a gradual increase in air temperature with height (Lin et al. 2017).

The GMS_B is the integrated effect of $\partial_p h$ weighted by Ω. We can illustrate how the lower unstable und upper stable profiles lead to the total GMS_B by integrating from the surface to the tropopause, see Fig. 7c. In the lower part of the troposphere, until about 500 hPa, the unstable profile dominates leading to an integrated GMS that is unstable. This is even more unstable in the SSP scenario, due to the increased $\partial_p h$ at lower levels. Above 500 hPa the integrated GMS sharply turns into stable (positive) profiles due to the now stable $\partial_p h$ at higher levels. This turnaround is much sharper in the SSP scenario, due to the increase Ω, leading to an overall integrated GMS_B that is more stable than in the HIS scenario.

While the total change in GMS_B is a combined effect of changes in $\partial_p h$ and Ω, it is indeed primarily a result of the change in Ω. This can be illustrated if we repeat the integration of the GMS from the surface to the tropopause, by assuming h of the HIS scenario and Ω from the SSP scenario, thus just considering change in Ω, see green profile in Fig. 7c. This effect is what leads to the strong weakening of the tropical circulation when the MSEB model is integrated with just the changes in Ω (Fig. 6).

Figure 8a shows how the change in Ω affect the tropical circulation. It weakens the circulation in the entire tropics, including convective and non-convective regions, and is

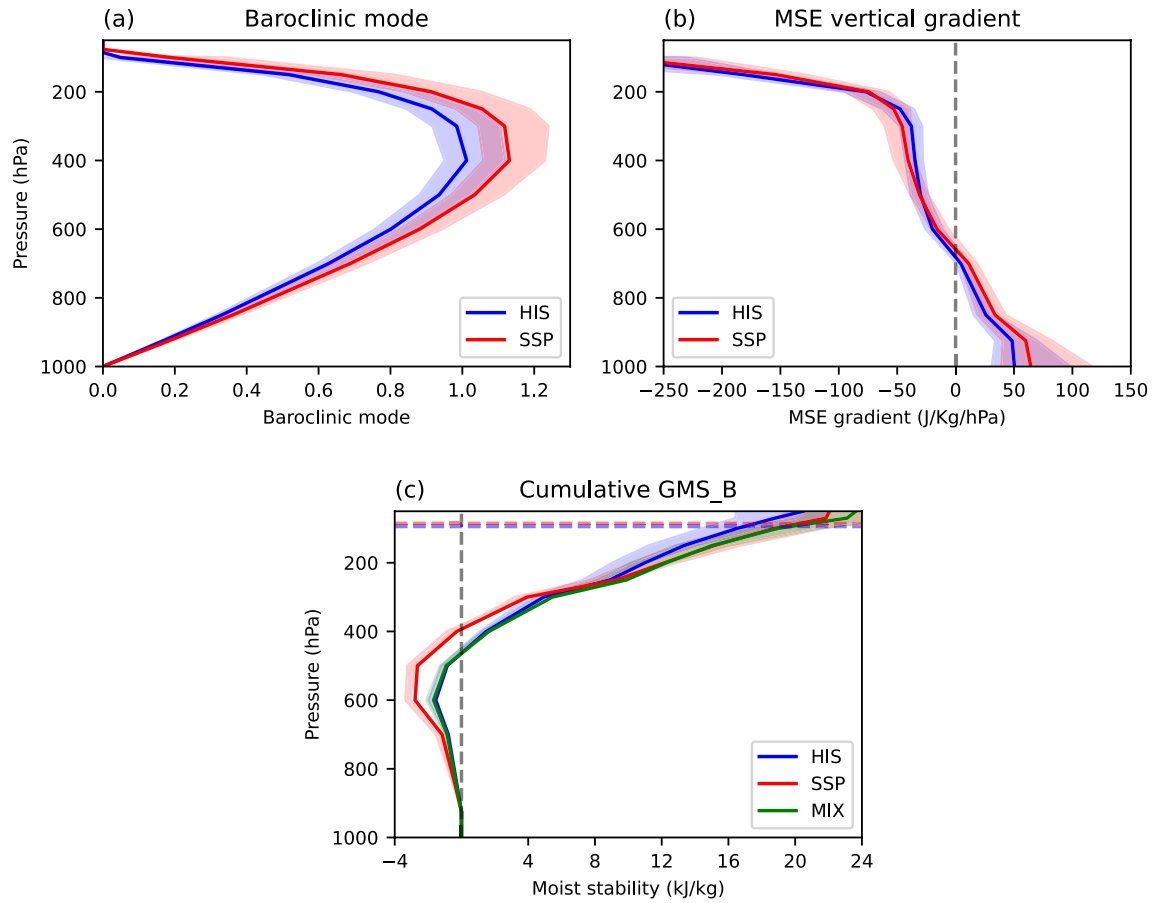

Fig. 7 Ensemble mean of the vertical profile based on 31 CMIP6 model outputs over the tropical ocean: **a** baroclinic mode, **b** vertical MSE pressure gradient, and **c** cumulative column-integrated GMS. The coloured lines represent the median of 31 climate model outputs in different scenarios (see the legend of each figure). The colour-filled region indicates a region between the minimum value and maximum value along with the x-axis. The green line in panel c (MIX) is the integration of the GMS from the surface to the tropopause, by assuming h of the HIS scenario (blue line in panel b) and baroclinic mode (Ω) from the SSP scenario (red line in panel a)

particularly significant over convective regions such as the Indo-Pacific warm pool, the Intertropical Convergence Zone and South Pacific Convergence Zone, the subtropical Atlantic, and the eastern equatorial Atlantic. The changes due to the baroclinic mode closely resembles the findings of Wills et al. (2017). The changes in $\partial_p h$ have a weaker impact on the tropical circulation and are opposite to those of the Ω effects (Fig. 8b). The increased instability at the lower levels of the troposphere mostly affect the deep tropics, by enhancing the circulation there. The impact on the subtropical regions is weaker and less clear.

4.4 Changes of baroclinic mode and the lifting of the tropopause height

We have illustrated above that the weakening of the tropical circulation is driven by the changes in the baroclinic mode, Ω. In the framework of the MSEB model Ω can change due to a change in the mean tropical temperature profile or due to a change in tropopause height, P_T. The sensitivity of the RMS of the tropical circulation in the MSEB model to both of these changes for the estimation of Ω are shown in Fig. 9. The changes in the temperature profile have only a very small effect on Ω and only weaken tropical circulation slightly. In turn, the change in P_T is the primary cause of the change in Ω and in the weakening of the tropical circulation. In the temperature profile sensitivity estimate, we calculate the baroclinic mode using the temperature profile of the SSP scenario while keeping the tropopause height fixed at the HIS scenario. Conversely, in the tropopause sensitivity estimate, we solely substitute P_T from the HIS scenario with P_T from the SSP scenario for the calculation of the baroclinic mode.

Figure 10 displays the baroclinic mode structure observed in the corresponding sensitivity experiments. The results provide clear evidence that the shift in Ω (Fig. 7a) is primarily attributed to changes in tropopause height under the warming scenario, rather than the temperature profile. Based

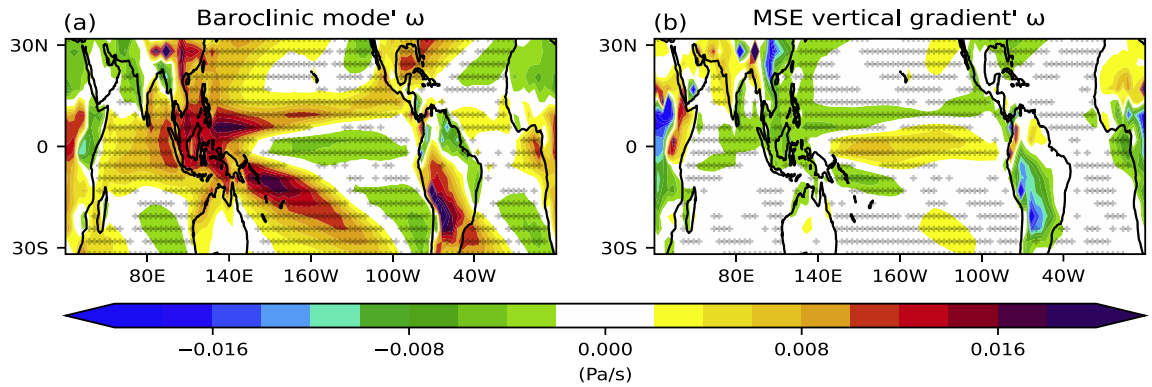

Fig. 8 MSEB model sensitivity of ω to changes in the baroclinic mode (Ω; left) and changes in MSE (right). The stippling indicates that over 22 (70%) CMIP6 models agree with the change of the sign

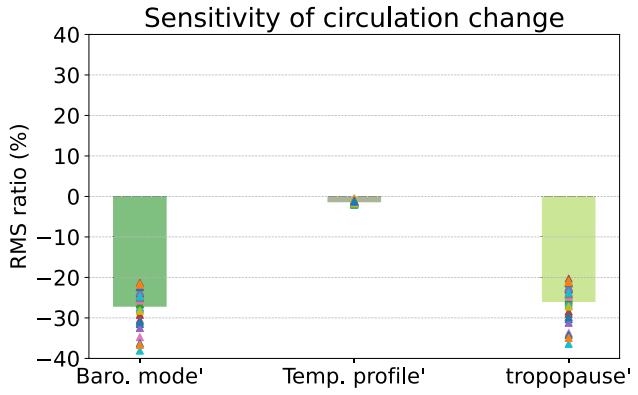

Fig. 9 Ensemble mean changes in the RMS of ω for the tropical ocean based on the sensitivity experiments (see x-axis labels). The detailed sensitivity method is described in Sect. 2.3. The symbol of the triangle represents each individual climate model

on the Ω observed in the tropopause height experiment (Fig. 10b), our findings (not shown) further suggest that the weakening circulation resulting from changes in tropopause height is due to the alterations in the weight carried by Ω. In turn, changes in the integral level for the new tropopause height have only a small effect that would strengthen the circulation slightly.

The change in the tropical mean temperature profile and tropopause height over oceans in the CMIP6 ensemble are shown in Fig. 11a and b, respectively. It clearly depicts a rising of the tropopause height under a warming scenario in all model simulations. It rises from about 97 hPa to 80 hPa by the end of the twenty-first century, consistent with previous studies (Santer et al. 2003; Seidel and Randel 2006; Vallis et al. 2015). The MSEB model assumes a tropical mean tropopause height, thus does not consider regional different. Figure 11c and d show the mean tropopause height and its change, respectively. We can note, that to first order

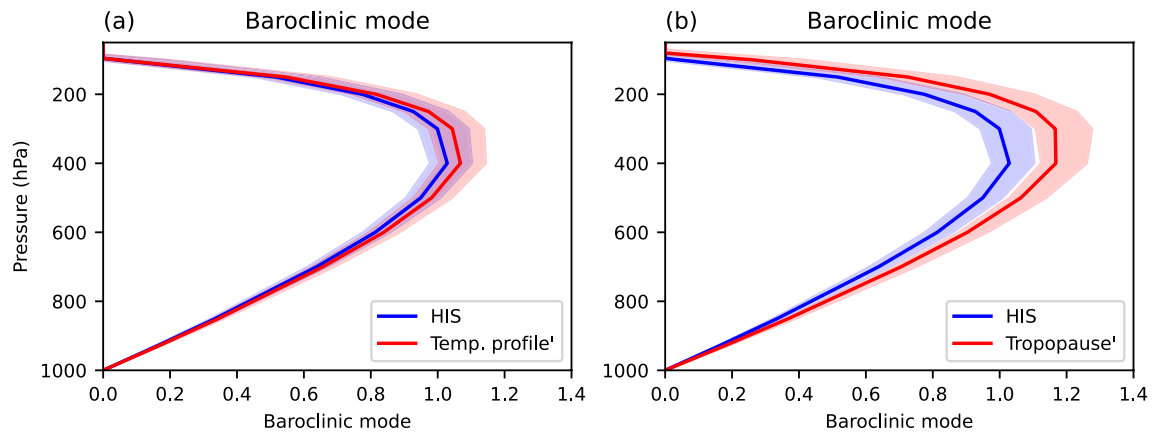

Fig. 10 Ensemble mean of the baroclinic mode (historical scenario vs. sensitivity experiment) based on 31 CMIP6 model outputs over the tropical ocean: **a** sensitivity experiment of temperature profile and **b** sensitivity experiment of tropopause height. The colored lines represent the median of 31 climate model outputs in different cases (see the legend of each figure). The color-filled region indicates a region between the minimum value and maximum value along with the x-axis

the tropopause height is indeed very similar throughout the tropics and the lifting of the tropopause height is similar throughout the tropics as well. This suggests that the MSEB model approximation of a tropical mean tropopause height is a reasonable simplification.

5 Summary and discussion

In this study we analyzed the weakening of the tropical circulation, as simulated in the CMIP6 model ensemble. We found that the tropical circulation weakens by the end of the century by about 10–15% relative to middle of the previous century (Kjellsson 2015; Huang et al. 2017), with a stronger and clearer signal over oceans than over land. This weakening of the circulation represents about 32% of the total change in the circulation, suggesting that about 68% of the change in the tropical circulation is due to change in the spatial pattern of the large-scale vertical motion.

We used the MSEB model to understand what is causing the overall weakening of the tropical circulation. The MSEB model diagnoses the tropical circulation (vertical motion) by the combined effect net heating and advection of moisture or heat where the sensitivity to these two terms is controlled by gross moist stability with an assumption of a first-order baroclinic mode. The MSEB model has good skills in presentation of the large-scale circulation and its change over tropical oceans, but has some limitations over land.

We evaluated the sensitivity of the tropical circulation changes to all main elements of the MSEB model to find the cause of the weakening of the tropical circulation. The tropical-wide weakening of the circulation can clearly be related to the lifting of the tropopause height (Chou and Chen 2010; Chou et al. 2013; Wills et al. 2017). While, changes in other aspects of the MSEB model also do lead to substantial changes in the tropical circulation, these changes are regionally quite different and overall lead to a strengthening of the circulation (Su et al. 2014; Long et al. 2016), counteracting the overall weakening of the circulation caused by the lifting of the tropopause height. The lifting of the tropopause height alone would approximately lead to a twice as strong weakening of the tropical circulation.

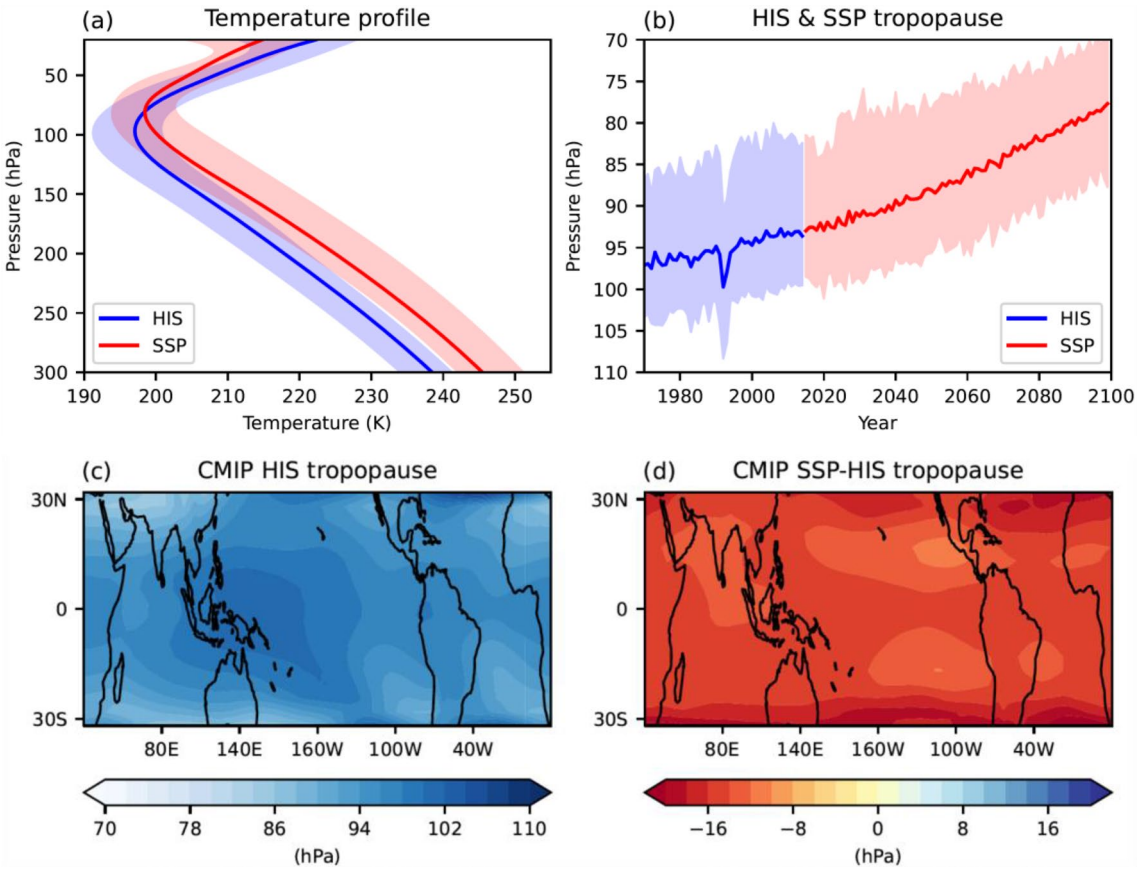

Fig. 11 **a** Upper tropospheric temperature profile and **b** Time series (1970–2099) of the tropopause height based on 31 CMIP6 model outputs over the tropics. Coloured lines represent the ensemble mean. The colour-filled region indicates a region between the minimum value and maximum value along with the y-axis. **c** Annual mean tropopause height in the historical scenario (1970–1999). **d** Tropopause height change from SSP5-8.5 warming scenario (2070–2099) data minus historical scenario data

In Fig. 12 we conceptually summarize how the overall weakening of the tropical circulation, due to the rise of the tropopause height, comes about. As a starting point we can consider the response to carbon dioxide forcing in an air column, which is in radiative and convective equilibrium (Manabe and Wetherald 1967). This provides a concept which does not involve any large-scale circulation yet. In this framework the increased heating in the atmosphere by the increased carbon dioxide leads to a homogenous warming of the troposphere and a cooling in the stratosphere very similar to the temperature profile changes found in the CMIP simulations (Fig. 12 Step I). This contrast in warming and cooling between the troposphere and stratosphere leads to a lifting of the tropopause height.

The lifting of the tropopause height leads to an expansion of the first baroclinic mode to higher levels and an increase in the strength of the mode at higher levels of the troposphere (Fig. 12 Step II) (Wills et al. 2017). The moist static stability in these higher levels of the tropical troposphere is dominated by stable air masses, in contrast to the lower levels of the atmosphere that are dominated by unstable air masses (Fig. 12 Step III).

The strength of the vertical motion in the tropical troposphere is the vertically integrated effect of the gross moist stability weighted by the first baroclinic mode (Eq. 3). While the gross moist stability becomes more unstable, supporting an intensification of the tropical circulation, the upward shift of the first baroclinic mode shifts the weighting of the stability into dryer and more stable atmospheric profiles, leading to an overall weaker, but higher reaching circulation (Fig. 12 Step IV).

The weakening of the tropical circulation is of fundamental importance for understanding tropical precipitation changes. It mutes some aspects of the large-scale precipitation response from 7% per degree warming, as it would follow from the Clausius Clapeyron relationship, to just

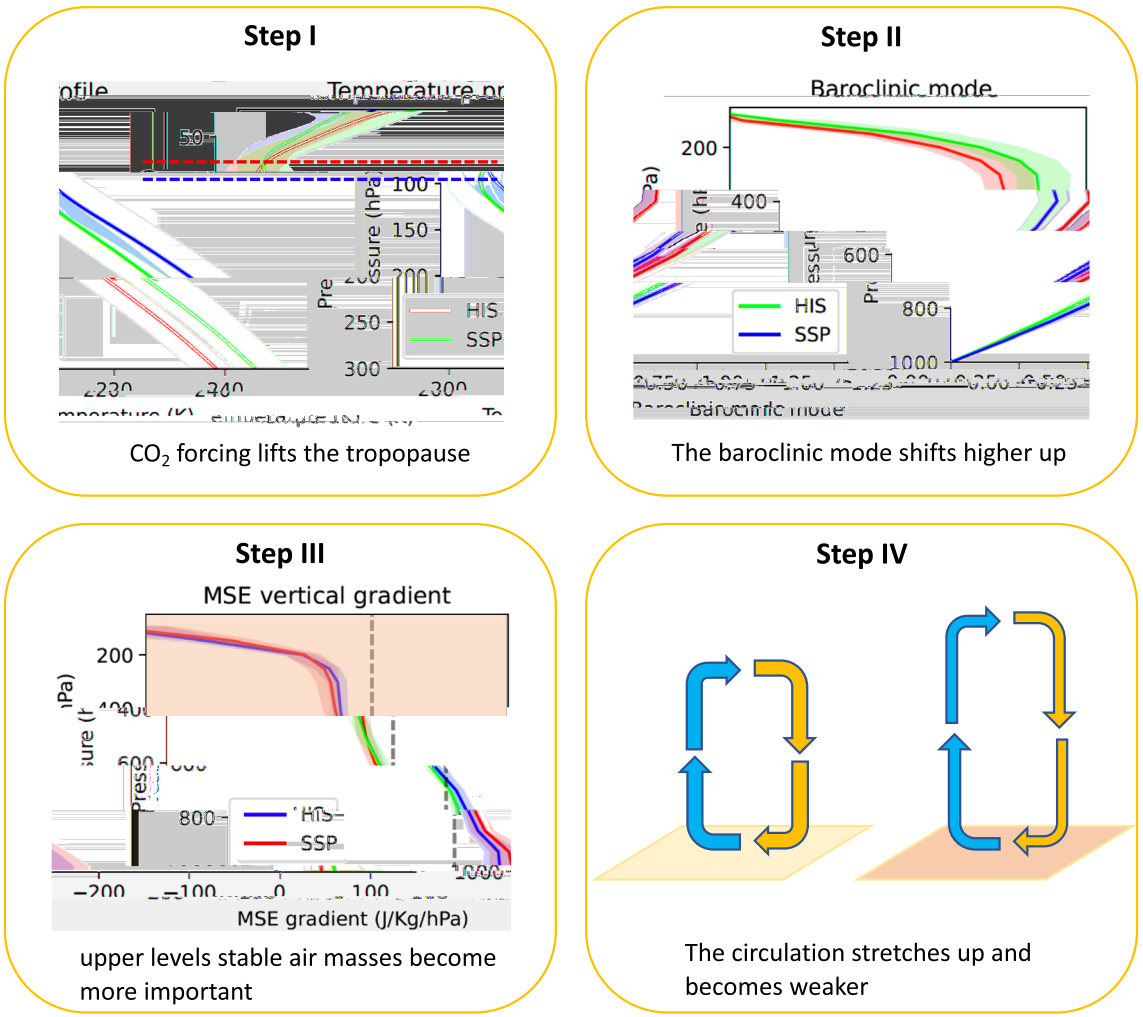

Fig. 12 Conceptual synthesis. Panel 1 is a recap of Fig. 11. Panel 2 and 3 are recaps of Fig. 7, and the final panel is an idealized sketch of the circulation changes

2–3% per degree warming (Held and Soden 2006; Wills et al. 2016). The clear link between the lifting of the tropopause height and the weakening of the tropical circulation, implies that precipitation changes, on the large-scale are also directly related to the lifting of the tropopause height. This may have implications on the precipitation response in different scenarios that, for instance, consider forcings alternative to carbon dioxide (e.g., solar radiation management, aerosols, etc.). Such alternative forcings can have a different impact on the tropopause height (Santer et al. 2003), and therefore can lead to different precipitation response. Thus, studies aiming at understanding large-scale precipitation response to different forcings, such as used in geo-engineering studies (Schmidt et al. 2012), should focus on the changes in tropopause height, as this will have a strong controlling effect on large-scale precipitation.

The results found here for the CMIP6 simulations using the MSEB model are robust and give a clear signal. However, there are a number of limitations and open questions that need to be pointed out, which should motivate further studies. First, despite the good approximation of the MSEB model, it does have some limitations over land, but also over oceans. It, for instance, assumes a uniform first baroclinic mode for all tropical regions. This is a simplification, that holds less over dryer regions and at higher latitudes. The definition of the tropopause height can also affect the outcome of the MSEB model to some degree. Further studies should approach these problems to evaluate how these would affect the outcomes.

Further, it must be stressed here that the study is entirely based on CMIP6 model simulations. To what extend the observed changes in the tropical circulation do follow the same mechanism has not been evaluated. Indeed, recent trends in the tropical Pacific suggest a strengthening of the Walker circulation (Bayr et al. 2014; Wills et al. 2022; Heede and Fedorov 2023), which is in strong contrast to what CMIP model simulations suggest. If such observed trends are a response to carbon dioxide forcing, they could suggest that the weakening of the tropical circulation is not as dominant as the CMIP6 simulations suggest, but that other processes that cause a strengthening of the tropical circulation are more important. It requires further studies into the recent observed trends to evaluate this.

While the study here focused on the weakening of the tropical circulation, the results also indicated significant other changes in the large-scale tropical circulation that can be diagnosed with the MSEB model. Further studies of the CMIP6 simulations and the observed tropical circulation changes should be conducted using a similar MSEB model-based approach to gain further understanding on what is causing other important changes in the tropical circulation.

Acknowledgements This research is based on the Chen-Shuo Fan's doctoral thesis, titled "[Conceptual understanding of the drivers of the large-scale tropical circulation]." We thank Paul O'Gorman and Sarah M. Kang for valuable feedback. We thank Robert Jnglin Wills and one anonymous reviewer for very thoughtful feedback which improved the paper. This study was supported by the Australian Research Council (ARC), ARC Centre of Excellence for Climate Extremes (Grant No. CE170100023). The research was undertaken with the assistance of resources and services from the National Computational Infrastructure (NCI), which is supported by the Australian Government.

Funding Open Access funding enabled and organized by CAUL and its Member Institutions. This study was supported by the Australian Research Council (ARC), ARC Centre of Excellence for Climate Extremes (Grant No. CE170100023).

Data availability All historical and SSP5-8.5 warming scenarios data for the 32 CMIP6 models used during this study are openly available from the Earth System Grid Federation at https://esgf-node.llnl.gov/search/cmip6/.

Declarations

Conflict of interest The authors have no relevant financial or non-financial interests to disclose.

References

Bayr T, Dommenget D, Martin T, Power SB (2014) The eastward shift of the Walker circulation in response to global warming and its relationship to ENSO variability. Clim Dyn 43:2747–2763. https://doi.org/10.1007/s00382-014-2091-y

Bony S, Bellon G, Klocke D et al (2013) Robust direct effect of carbon dioxide on tropical circulation and regional precipitation. Nat Geosci 6:447–451. https://doi.org/10.1038/ngeo1799

Byrne MP, Schneider T (2016) Narrowing of the ITCZ in a warming climate: physical mechanisms. Geophys Res Lett 43(11):311–350. https://doi.org/10.1002/2016GL070396

Chemke R, Polvani LM (2021) Elucidating the mechanisms responsible for Hadley cell weakening under $4 \times CO_2$ forcing. Geophys Res Lett. https://doi.org/10.1029/2020GL090348

Chou C, Chen C-A (2010) Depth of convection and the weakening of tropical circulation in global warming. J Clim 23:3019–3030. https://doi.org/10.1175/2010JCLI3383.1

Chou C, Neelin JD, Chen C-A, Tu J-Y (2009) Evaluating the "Rich-Get-Richer" mechanism in Tropical precipitation change under global warming. J Clim 22:1982–2005. https://doi.org/10.1175/2008JCLI2471.1

Chou C, Wu TC, Tan PH (2013) Changes in gross moist stability in the tropics under global warming. Clim Dyn 41:2481–2496. https://doi.org/10.1007/s00382-013-1703-2

DiNezio PN, Vecchi GA, Clement AC (2013) Detectability of changes in the Walker circulation in response to global warming. J Clim 26:4038–4048. https://doi.org/10.1175/JCLI-D-12-00531.1

Duffy ML, O'Gorman PA (2023) Intermodel spread in Walker circulation responses linked to spread in moist stability and radiation responses. J Geophys Res Atmos. https://doi.org/10.1029/2022JD037382

Eyring V, Bony S, Meehl GA et al (2016) Overview of the coupled model Intercomparison Project Phase 6 (CMIP6) experimental design and organization. Geosci Model Dev 9:1937–1958. https://doi.org/10.5194/gmd-9-1937-2016

Fan C-S, Dommenget D (2021) A diagnostic model for the large-scale tropical circulation based on moist static energy balance. Clim Dyn 57:3159–3181. https://doi.org/10.1007/s00382-021-05861-2

Feldl N, Bordoni S (2016) Characterizing the Hadley circulation response through regional climate feedbacks. J Clim 29:613–622. https://doi.org/10.1175/JCLI-D-15-0424.1

Gettelman A, Birner T, Eyring V et al (2009) The tropical tropopause layer 1960–2100. Atmos Chem Phys 9:1621–1637. https://doi.org/10.5194/acp-9-1621-2009

Heede UK, Fedorov AV (2023) Colder eastern equatorial Pacific and stronger Walker circulation in the early 21st century: separating the forced response to global warming from natural variability. Geophys Res Lett. https://doi.org/10.1029/2022GL101020

Held IM, Soden BJ (2006) Robust responses of the hydrological cycle to global warming. J Clim 19:5686–5699. https://doi.org/10.1175/JCLI3990.1

Hu Y, Huang H, Zhou C (2018) Widening and weakening of the Hadley circulation under global warming. Sci Bull (Beijing) 63:640–644. https://doi.org/10.1016/j.scib.2018.04.020

Huang P, Chen D, Ying J (2017) Weakening of the tropical atmospheric circulation response to local sea surface temperature anomalies under global warming. J Clim 30:8149–8158. https://doi.org/10.1175/JCLI-D-17-0171.1

IPCC (2021) Climate change 2021: the physical science basis. Contribution of Working Group I to the Sixth Assessment Report of the Intergovernmental Panel on Climate Change. In: Masson-Delmotte V, Zhai P, Pirani A, Connors SL, Péan C, Berger S, Caud N, Chen Y, Goldfarb L, Gomis MI, Huang M, Leitzell K, Lonnoy E, Matthews JBR, Maycock TK, Waterfield T, Yelekçi O, Yu R, Zhou B (eds). Cambridge University Press, Cambridge, United Kingdom and New York, NY, USA

Kim D, Kim H, Kang SM et al (2022) Weak Hadley cell intensity changes due to compensating effects of tropical and extratropical radiative forcing. NPJ Clim Atmos Sci 5:61. https://doi.org/10.1038/s41612-022-00287-x

Kjellsson J (2015) Weakening of the global atmospheric circulation with global warming. Clim Dyn 45:975–988. https://doi.org/10.1007/s00382-014-2337-8

Lin P, Paynter D, Ming Y, Ramaswamy V (2017) Changes of the tropical tropopause layer under global warming. J Clim 30:1245–1258. https://doi.org/10.1175/JCLI-D-16-0457.1

Long S-M, Xie S-P, Liu W (2016) Uncertainty in tropical rainfall projections: atmospheric circulation effect and the ocean coupling. J Clim 29:2671–2687. https://doi.org/10.1175/JCLI-D-15-0601.1

Manabe S, Wetherald RT (1967) Thermal equilibrium of the atmosphere with a given distribution of relative humidity. J Atmos Sci 24:241–259. https://doi.org/10.1175/1520-0469(1967)024%3c0241:TEOTAW%3e2.0.CO;2

Mitas CM, Clement A (2006) Recent behavior of the Hadley cell and tropical thermodynamics in climate models and reanalyses. Geophys Res Lett. https://doi.org/10.1029/2005GL024406

O'Neill BC, Tebaldi C, van Vuuren DP et al (2016) The scenario Model Intercomparison Project (ScenarioMIP) for CMIP6. Geosci Model Dev 9:3461–3482. https://doi.org/10.5194/gmd-9-3461-2016

Plesca E, Buehler SA, Grützun V (2018) The fast response of the tropical circulation to CO2 forcing. J Clim 31:9903–9920. https://doi.org/10.1175/JCLI-D-18-0086.1

Plesca E, Grützun V, Buehler SA (2018) How robust is the weakening of the Pacific Walker circulation in CMIP5 idealized transient climate simulations? J Clim 31:81–97. https://doi.org/10.1175/JCLI-D-17-0151.1

RAND Corporation (1980) Rand's global elevation and depth data. https://doi.org/10.5065/HKKR-P122. Accessed 8 Mar 2023

Richter I, Xie S-P (2008) On the origin of equatorial Atlantic biases in coupled general circulation models. Clim Dyn 31:587–598. https://doi.org/10.1007/s00382-008-0364-z

Santer BD, Wehner MF, Wigley TML et al (2003) Contributions of anthropogenic and natural forcing to recent tropopause height changes. Science 301:479–483. https://doi.org/10.1126/science.1084123

Schmidt H, Alterskjær K, Bou Karam D et al (2012) Solar irradiance reduction to counteract radiative forcing from a quadrupling of CO_2: climate responses simulated by four earth system models. Earth Sys Dyn 3:63–78. https://doi.org/10.5194/esd-3-63-2012

Seidel DJ, Randel WJ (2006) Variability and trends in the global tropopause estimated from radiosonde data. J Geophys Research: Atmos. https://doi.org/10.1029/2006JD007363

Singh MS, O'Gorman PA (2012) Upward shift of the atmospheric general circulation under global warming: theory and simulations. J Clim 25:8259–8276. https://doi.org/10.1175/JCLI-D-11-00699.1

Su H, Jiang JH, Zhai C et al (2014) Weakening and strengthening structures in the Hadley circulation change under global warming and implications for cloud response and climate sensitivity. J Geophys Res: Atmos 119:5787–5805. https://doi.org/10.1002/2014JD021642

Tokinaga H, Xie S-P, Deser C et al (2012) Slowdown of the Walker circulation driven by tropical Indo-Pacific warming. Nature 491:439–443. https://doi.org/10.1038/nature11576

Vallis GK, Zurita-Gotor P, Cairns C, Kidston J (2015) Response of the large-scale structure of the atmosphere to global warming. Q J R Meteorol Soc 141:1479–1501. https://doi.org/10.1002/qj.2456

Vecchi GA, Soden BJ (2007) Global warming and the weakening of the tropical circulation. J Clim 20:4316–4340. https://doi.org/10.1175/JCLI4258.1

Wills RC, Byrne MP, Schneider T (2016) Thermodynamic and dynamic controls on changes in the zonally anomalous hydrological cycle. Geophys Res Lett. https://doi.org/10.1002/2016GL068418

Wills RC, Dong Y, Proistosecu C et al (2022) Systematic climate model biases in the large-scale patterns of recent sea-surface temperature and sea-level pressure change. Geophys Res Lett. https://doi.org/10.1029/2022GL100011

Wills RC, Levine XJ, Schneider T (2017) Local energetic constraints on walker circulation strength. J Atmos Sci 74:1907–1922. https://doi.org/10.1175/JAS-D-16-0219.1

Wu M, Zhou T, Li C et al (2021) A very likely weakening of Pacific Walker circulation in constrained near-future projections. Nat Commun 12:6502. https://doi.org/10.1038/s41467-021-26693-y

Xia Y, Hu Y, Liu J (2020) Comparison of trends in the Hadley circulation between CMIP6 and CMIP5. Sci Bull (Beijing) 65:1667–1674. https://doi.org/10.1016/j.scib.2020.06.011

Xie S-P, Deser C, Vecchi GA et al (2010) Global warming pattern formation: sea surface temperature and rainfall. J Clim 23:966–986. https://doi.org/10.1175/2009JCLI3329.1